

---

# HIGHLY OVER-PARAMETERIZED CLASSIFIERS GENERALIZE SINCE BAD SOLUTIONS ARE RARE

---

A PREPRINT

**Julius Martinetz**  
Machine Learning Group  
Technical University Berlin  
Berlin, Germany  
j.martinetz@tu-berlin.de

**Thomas Martinetz**  
Institute for Neuro- and Biocomputing  
University of Lübeck  
Lübeck, Germany  
martinetz@inb.uni-luebeck.de

May 25, 2023

## ABSTRACT

We study over-parameterized classifiers where Empirical Risk Minimization (ERM) for learning leads to zero training error. In these over-parameterized settings there are many global minima with zero training error, some of which generalize better than others. We show that under certain conditions the fraction of "bad" global minima with a true error larger than  $\varepsilon$  decays to zero exponentially fast with the number of training data  $n$ . The bound depends on the distribution of the true error over the set of classifier functions used for the given classification problem, and does not necessarily depend on the size or complexity (e.g. the number of parameters) of the classifier function set. This might explain the unexpectedly good generalization even of highly over-parameterized Neural Networks. We validate our mathematical framework with experiments on a synthetic data set and a subset of MNIST, and also test our hypothesis with VGG19 and ResNet18 on a subset of Caltech101.

## 1 Introduction

Extreme upscaling and deepening of Neural Networks has led to a quantum leap in many real-world object recognition tasks [1]. The same is true for Neural Networks in Natural Language Processing [2] and reinforcement learning [3]. By enlarging the networks appropriately, the level of performance increases, and even entering regimes with many more network parameters than training samples does not harm generalization. This is usually attributed to an appropriate regularization. However, generalization is also observed in highly over-parameterized regimes and without explicit regularization, where even random label assignments or even random image data can be memorized [4]. Belkin called this the "modern" interpolation regime' [5].

The generalization capabilities of large Neural Networks do not seem to be harmed by the millions of parameters in today's popular architectures. Due to their large, inherent capacity the training error is zero after training by Empirical Risk Minimization (ERM), i.e. the training data is memorized. Nevertheless, the test error can be unexpectedly low [4], even after only a few handful of training samples [6]. This is in contrast to traditional machine learning wisdom, where one would not expect any generalization in these highly over-parameterized regimes, where the data is highly over-fitted. Statistical learning theory based on uniform generalization bounds requires a high probability that there is no solution with a large deviation between empirical and expected risk, i.e. the training and the true error. However, this is not the case in over-parameterized regimes. There is no uniform generalization bound. In these highly over-parameterized regimes always also "bad" solutions with zero training but large true error do exist. Interestingly, they hardly seem to occur in practice.

In this paper, we investigate over-parameterized classifiers with training error zero after training. A classifier receives inputs  $x$  from an input distribution  $P(x)$  and assigns a class label using a classifier function  $h(x)$ . The input  $x$  has a true label  $y$  with probability  $P(y|x)$ . For each input  $x$ , the classifier produces a loss  $L(y, h(x)) \in \{0, 1\}$ , 0 if the classification is correct and 1 if the classification is incorrect. The error of the classifier  $h$  on the whole data distribution

$P(x, y) = P(y|x)P(x)$  is given by the expected loss

$$E(h) = \int L(y, h(x))P(x, y)dx dy.$$

$E(h)$  always lies between 0 and 1 and is also called true error, expected loss or risk.

The classifier or predictor  $h$  is usually chosen from a function set  $\mathcal{H}$ . For example,  $\mathcal{H}$  is determined by the architecture of a Neural Network, and the allocated  $h$  is determined by the network parameters. Learning means selecting an  $h$  from the set  $\mathcal{H}$  so as to minimize  $E(h)$ . This is often done by Empirical Risk Minimization (ERM). Let  $\mathcal{S} = \{(x_1, y_1), \dots, (x_n, y_n)\}$  be a so-called training set of  $n$  input samples  $x$  together with their labels  $y$  which are independently drawn from  $P(x, y)$ . Empirical risk is defined as the average loss on this training set

$$E_{\mathcal{S}}(h) = \frac{1}{n} \sum_{i=1}^n L(y_i, h(x_i)).$$

$E_{\mathcal{S}}(h)$  is also variously referred to as the training error or empirical loss. Learning via ERM chooses an  $h \in \mathcal{H}$  that minimizes  $E_{\mathcal{S}}(h)$ . However,  $E(h)$  and  $E_{\mathcal{S}}(h)$  may deviate. This deviation is called the generalization gap.

If the generalization gap is small, a small training error provides a good solution with a small true error. Statistical learning theory, e.g., based on VC-dimension [7] or Rademacher complexity [8], provides bounds for the generalization gap by uniform convergence. With uniform convergence, the generalization gap becomes small with increasing  $n$  for each  $h \in \mathcal{H}$ . "Bad" solutions with large generalization gaps are ruled out with high probability. However, these bounds do not exist in highly over-parameterized regimes. There are always  $h \in \mathcal{H}$  left with large generalization gaps. Nevertheless, in practice learning takes place and ERM provides good solutions that generalize well also in these over-parameterized regimes. There have been theoretical and empirical attempts to understand this "mystery". It has been argued, that this might be due to implicit regularization of (stochastic) gradient descent [9], [10], [11]. A number of novel algorithmic-dependent uniform generalization bounds based on norm or compression measures have been supposed for explanation (e.g. [12], [13], [14], [15], [16], [17], [18], [19], [20], [21]). But still there is empirically based scepticism that these bounds already help [22] or that uniform convergence bounds in principle are the right approach [23].

In the following, we allow for "bad" classifiers. As long as its fraction within the set of global minima with zero training error is small, the ERM algorithm should easily be able to provide a good solution. This is much less than trying to enforce uniform generalization bounds, i.e., that the fraction of "bad" classifiers within the set of global minima is zero with high probability, and may help explain the "mystery" of good generalization in over-parameterized regimes.

## 2 Notations and theorem

We start with a discrete and finite function set  $\mathcal{H}$ . In fact, this is always the case if digital computers are used. If  $\mathcal{H}$  is parameterized by a continuous parameter space, then we discretize the parameter space appropriately.  $E_{min} = \min_{h \in \mathcal{H}} E(h)$  denotes the minimum true error of the classifier function set  $\mathcal{H}$  on the given classification problem. We work with the following subsets of  $\mathcal{H}$ :

$$\begin{aligned} \mathcal{H}_{\varepsilon} & : \text{ set of all classifiers } h \in \mathcal{H} \text{ with } E(h) \geq E_{min} + \varepsilon \quad (\varepsilon > 0) \\ \mathcal{H}(\mathcal{S}) & : \text{ set of all classifiers } h \in \mathcal{H} \text{ with } E_{\mathcal{S}}(h) = 0 \\ \mathcal{H}_{\varepsilon}(\mathcal{S}) & : \text{ set of all classifiers } h \in \mathcal{H}_{\varepsilon} \text{ with } E_{\mathcal{S}}(h) = 0 \end{aligned}$$

$\mathcal{H}(\mathcal{S})$  is the set of all global minima on the training error  $E_{\mathcal{S}}(h)$  for a given training set  $\mathcal{S}$ . The ERM algorithm ends up in one of these global minima<sup>1</sup>.  $\mathcal{H}_{\varepsilon}(\mathcal{S})$  is what we call the set of "bad" global minima with true errors larger than  $\varepsilon$ . Further, we use the notations  $H = |\mathcal{H}|$ ,  $H_{\varepsilon} = |\mathcal{H}_{\varepsilon}|$ ,  $H(\mathcal{S}) = |\mathcal{H}(\mathcal{S})|$  and  $H_{\varepsilon}(\mathcal{S}) = |\mathcal{H}_{\varepsilon}(\mathcal{S})|$  for the set sizes. In the following the fractions

$$\begin{aligned} g_{\varepsilon} = \frac{H - H_{\varepsilon}}{H} & : \text{ fraction of "good" classifiers within } \mathcal{H} \text{ with } E_{min} \leq E(h) \leq E_{min} + \varepsilon \\ b_{\varepsilon}(\mathcal{S}) = \frac{H_{\varepsilon}(\mathcal{S})}{H(\mathcal{S})} & : \text{ fraction of "bad" classifiers within the set of global minima } \mathcal{H}(\mathcal{S}) \end{aligned}$$

are important.  $g_{\varepsilon}$  as the fraction of "good" classifiers within the classifier function set  $\mathcal{H}$  is a measure for the "appropriateness" of  $\mathcal{H}$  for the given classification problem. It is a measure for the bias of the classifier function set.

<sup>1</sup>Convergence to global minima of ERM algorithms such as gradient descent or its variants is a topic on its own rights. However, in highly over-parameterized settings convergence to zero training error is usually not a problem.

$b_\varepsilon(\mathcal{S})$  is the main property we are looking at. We show that under certain conditions  $b_\varepsilon(\mathcal{S})$  is likely to become small with increasing  $n$  and relate it to  $g_\varepsilon$ . If  $b_\varepsilon(\mathcal{S})$  is small, it is easier for the ERM algorithm to end up in a good solution.

This leads to the following statements, for which the short proofs are given in the Appendix:

**Lemma 1.** *Let  $\langle H_\varepsilon(\mathcal{S}) \rangle$  be the size of  $\mathcal{H}_\varepsilon(\mathcal{S})$  averaged over all training sets of size  $n$ , then for each  $0 \leq \varepsilon \leq 1 - E_{min}$*

$$\langle H_\varepsilon(\mathcal{S}) \rangle = \sum_{h \in \mathcal{H}_\varepsilon} (1 - E(h))^n \leq H_\varepsilon (1 - (E_{min} + \varepsilon))^n \quad (1)$$

$\langle H_\varepsilon(\mathcal{S}) \rangle$  gives us the mean set size of "bad" global minima which lead to "bad" solutions with a true error worse than  $E_{min} + \varepsilon$ . Lemma 1 tells us, that for each  $\varepsilon > 0$ , the mean set size of "bad" global minima decreases to zero exponentially fast with increasing  $n$ .

The mean set size  $\langle H(\mathcal{S}) \rangle$  of all global minima is given by (1) for  $\varepsilon = 0$  and also converges exponentially, either to zero in case  $E_{min} > 0$ , or to the number of solutions with true error zero in case  $E_{min} = 0$ . However, it converges much slower than the mean set size of "bad" global minima.

**Corollary 1.** *For each  $0 < \varepsilon \leq 1 - E_{min}$*

$$\frac{\langle H_\varepsilon(\mathcal{S}) \rangle}{\langle H(\mathcal{S}) \rangle} \leq \frac{1}{g_{\varepsilon/2}} e^{-\frac{\varepsilon}{2}n}. \quad (2)$$

The quotient on the l.h.s. diminishes at least exponentially fast with  $n$ . Note, that the prefactor is determined by the inverse of the fraction of "good" classifiers within the function set  $\mathcal{H}$  (better than  $\varepsilon/2$ ) and, hence, becomes smaller with a better bias. It does not depend on the absolute number of classifier functions and does not increase necessarily with  $H$ , e.g., with the number of parameters. We will demonstrate this in experiments. The exponent is linear in  $\varepsilon$ .

Not the ratio of the mean set sizes, but  $b_\varepsilon(\mathcal{S}) = H_\varepsilon(\mathcal{S})/H(\mathcal{S})$  for a given  $\mathcal{S}$  has to be small to make it more likely for the ERM algorithm to end up in a "good" than in a "bad" solution. We show that this can be expected, if this fraction  $b_\varepsilon(\mathcal{S})$  of "bad" solutions within the set of all global minima does not correlate negatively with the set size of all global minima  $H(\mathcal{S})$ .

**Theorem 1.** *Given a training data set  $\mathcal{S}$ . If  $H(\mathcal{S}) > 0$  and if  $b_\varepsilon(\mathcal{S})$  does not correlate negatively with  $H(\mathcal{S})$  for randomly chosen  $\mathcal{S}$  with  $H(\mathcal{S}) > 0$ , then for each  $\gamma > 0$*

$$\text{Prob} \{b_\varepsilon(\mathcal{S}) \geq \gamma\} \leq \frac{1}{\gamma g_{\varepsilon/2}} e^{-\frac{\varepsilon}{2}n}.$$

The probability, that the fraction  $b_\varepsilon(\mathcal{S})$  of "bad" ERM solutions within the set of all ERM solutions is not small (smaller than  $\gamma$ ) for a given  $\mathcal{S}$ , decreases exponentially fast to zero with the number of training data  $n$ . "Bad" solutions become rare. For highly over-parameterized classifiers,  $H(\mathcal{S}) > 0$  is usually given. With  $\delta$  being the probability we want to achieve for  $b_\varepsilon(\mathcal{S}) \geq \gamma$  being valid, we need at most

$$n \leq \frac{2}{\varepsilon} \left( \ln \frac{1}{\delta\gamma} + \ln \frac{1}{g_{\varepsilon/2}} \right)$$

training samples.

Exactly when the condition that there is no negative correlation between  $b_\varepsilon(\mathcal{S})$  and  $H(\mathcal{S})$  is met, remains to be shown and should depend on the classifier function set  $\mathcal{H}$  and the classification problem determined by  $P(x, y)$ . The fraction of "bad" solutions must not decrease (on average) with increasing global minima set sizes. In our experiments with synthetic data and MNIST, we can show, at least experimentally for the given settings, that indeed no correlation is visible.

We show in the proof of Theorem 1, that without correlation

$$\langle b_\varepsilon(\mathcal{S}) \rangle_{\hat{\mathcal{S}}} = \frac{\langle H_\varepsilon(\mathcal{S}) \rangle}{\langle H(\mathcal{S}) \rangle} \quad (3)$$

is valid, and without a negative correlation

$$\langle b_\varepsilon(\mathcal{S}) \rangle_{\hat{\mathcal{S}}} \leq \frac{\langle H_\varepsilon(\mathcal{S}) \rangle}{\langle H(\mathcal{S}) \rangle}. \quad (4)$$

$\hat{\mathcal{S}}$  denotes the set of all training data sets  $\mathcal{S}$  with  $H(\mathcal{S}) > 0$ . With the Markov-inequality and Corollary 1, Theorem 1 follows.

### 3 Density of Classifiers (DOC)

The bounds (1) and (2) can be refined with a new quantity which we call "density of classifiers" (DOC). For large classifier function sets, e.g., large deep networks, there are usually many classifier functions with a true error  $E(h)$  within an interval  $E \leq E(h) \leq E + \Delta E$ . We introduce  $D(E)$  as the density of classifiers (DOC) at true error  $E$  such that

$$H_\varepsilon = \int_{E_{min} + \varepsilon}^1 D(E) dE \quad \text{for each} \quad 0 \leq \varepsilon \leq 1 - E_{min}.$$

Analog to the "density of states (DOS)" at a certain energy in physical systems,  $D(E)dE$  counts the number of classifier functions ("states")  $h \in \mathcal{H}$  with  $E \leq E(h) \leq E + dE$ . For  $0 \leq E < E_{min}$ ,  $D(E) = 0$ . In the discrete case,  $D(E)$  is given by a sum of delta-distributions  $D(E) = \sum_{h \in \mathcal{H}} \delta(E - E(h))$ .

In the continuous case, i.e., if  $\mathcal{H}$  is a compact set within a continuous space of parameters  $W$  with a Lebesgue measure,  $H$  is now the volume of  $\mathcal{H}$ . If we discretize according to the Lebesgue measure, in the limit the sum in (1) becomes the Riemann integral

$$\langle H_\varepsilon(\mathcal{S}) \rangle = \int_{\mathcal{H}} (1 - E(W))^n dW. \quad (5)$$

$H_\varepsilon(\mathcal{S})$  is now the volume of the subspace  $\mathcal{H}_\varepsilon(\mathcal{S})$  of "bad" parameter settings within  $\mathcal{H}(\mathcal{S})$ , and the density of classifiers  $D(E)$  is now a continuous distribution.

In the discrete and the continuous case we obtain

$$\langle H_\varepsilon(\mathcal{S}) \rangle = \int_{E_{min} + \varepsilon}^1 (1 - E)^n D(E) dE.$$

If the fraction  $b_\varepsilon(\mathcal{S})$  of "bad" global minima does not correlate with the set size  $H(\mathcal{S})$  of all global minima, then according to (3)

$$\langle b_\varepsilon(\mathcal{S}) \rangle_{\mathfrak{S}} = \frac{\int_{E_{min} + \varepsilon}^1 (1 - E)^n D(E) dE}{\int_0^1 (1 - E)^n D(E) dE}. \quad (6)$$

If it does not correlate negatively, then according to (4)

$$\langle b_\varepsilon(\mathcal{S}) \rangle_{\mathfrak{S}} \leq \frac{\int_{E_{min} + \varepsilon}^1 (1 - E)^n D(E) dE}{\int_0^1 (1 - E)^n D(E) dE}. \quad (7)$$

The bound is determined solely by  $D(E)$ . Since  $D(E)$  occurs in the nominator and denominator, it is not the absolute number (density) of classifiers, which determines the bound, but only the shape of  $D(E)$ , i.e.,  $D(E)$  up to a constant factor. As we will see later in our experiments, the shape of  $D(E)$  does not necessarily depend on the number of parameters of our classifier functions.

For all  $\mathcal{S}$  with  $H(\mathcal{S}) > 0$ , we define  $Q_{\mathcal{S}}(E)$  such that

$$\frac{H_\varepsilon(\mathcal{S})}{H(\mathcal{S})} = \int_{E_{min} + \varepsilon}^1 Q_{\mathcal{S}}(E) dE \quad \text{for each} \quad 0 \leq \varepsilon \leq 1 - E_{min}. \quad (8)$$

$Q_{\mathcal{S}}(E)$  is the normalized density of global minima at true error  $E$  for a given training data set  $\mathcal{S}$ . One will rather end up with a classifier at true errors where the density  $Q_{\mathcal{S}}(E)$  is large. With  $Q_n(E) := \langle Q_{\mathcal{S}}(E) \rangle_{\mathfrak{S}}$ , averaged over all  $\mathcal{S}$  with  $|\mathcal{S}| = n$  and  $H(\mathcal{S}) > 0$ , we obtain

$$\langle b_\varepsilon(\mathcal{S}) \rangle_{\mathfrak{S}} = \left\langle \frac{H_\varepsilon(\mathcal{S})}{H(\mathcal{S})} \right\rangle_{\mathfrak{S}} = \int_{E_{min} + \varepsilon}^1 Q_n(E) dE \quad \text{for each} \quad 0 \leq \varepsilon \leq 1 - E_{min}. \quad (9)$$

If (6) is valid, we have

$$Q_n(E) = \frac{(1 - E)^n D(E)}{\int_0^1 (1 - E)^n D(E) dE}. \quad (10)$$

The mean true error, averaged over the global minima of all  $\mathcal{S}$  with  $|\mathcal{S}| = n$  and  $H(\mathcal{S}) > 0$ , is then given by

$$\langle E_n \rangle_{\mathfrak{S}} = \int_0^1 E Q_n(E) dE. \quad (11)$$

## 4 Experiments

To experimentally verify our theoretical derivations, we study experimental setups in which we can determine  $D(E)$ ,  $H(\mathcal{S})$  and  $b_\varepsilon(\mathcal{S})$  by random sampling. We take multi-layer-perceptrons with leaky ReLUs (10% leakiness) and no bias. The output of the classifier is then given by

$$\mathbf{y} = \text{ReLU}(W_K \text{ReLU}(W_{K-1}(\dots \text{ReLU}(W_1 \mathbf{x}))))$$

with  $W_k$ ,  $k = 1, \dots, K$  as the weight matrix of layer  $k$ ,  $\mathbf{x} \in \mathbb{R}^D$  as the input vector of dimension  $D$  and  $\mathbf{y} \in \mathbb{R}^2$  as the output vector, in our case for binary classification. The ReLU of the output layer with the largest output determines the predicted class membership for the given input  $\mathbf{x}$ . In this setting, it is easy to see and well known that the class membership is invariant to the lengths of the weight vectors due to the positive homogeneity of the leaky ReLUs (for  $s \geq 0$ ,  $\text{ReLU}(sx) = s\text{ReLU}(x)$ ). Thus, each classifier function is determined by a weight vector (comprising all weights of the network) of unit length.  $\mathcal{H}$  is given by the unit sphere in dimension  $\mathbb{R}^N$ , with  $N$  as the number of weights of the network. In our experiments, we will sample uniformly from this unit sphere. With the leakiness of the ReLUs, we avoid too many trivial solutions with many "dead" ReLUs.

### 4.1 Synthetic data set

For the first experiment we take a synthetic data set of two isotropic Gaussians in 10 dimensions. The Gaussian of class A is centered at  $(+1, 0, \dots, 0)$  and of class B at  $(-1, 0, \dots, 0)$ . Both Gaussians have a variance of 0.5 and, hence, overlap with 2.28%. This is the minimal possible classification error  $E_{min}$ . We apply three different networks. The smallest has one hidden layer with ten hidden units, which leads to 120 weights. The next has again one hidden layer, but 100 hidden units, hence, with 1,200 ten times as many weights. The third network has ten hidden layers with ten units each, hence, 1,020 weights.

The first row of Fig. 1 shows the results with the smallest network. On the left we see its density of classifiers  $D(E)$  (up to a constant factor) as a histogram of 100 bins (A1). We determined  $D(E)$  by randomly sampling weight vectors from a uniform probability distribution on the 120-dimensional unit hypersphere. For each weight vector the true error of the corresponding classifier is measured with a balanced test set consisting of 10,000 randomly chosen test data from the two classes. The result is put into the corresponding bin. This was repeated 1,000,000 times. As expected,  $D(E)$  is symmetric and has its peak at  $E = 0.5$  and good classifiers with a small true error are rare within  $\mathcal{H}$ , i.e., on the hypersphere.

In a next step we probed the dependence of  $b_\varepsilon(\mathcal{S})$  on  $H(\mathcal{S})$ , how it correlates. We randomly drew different  $\mathcal{S}$  of the same size  $n = 10$ , and for each  $\mathcal{S}$  we repeatedly chose random weight vectors from the unit hypersphere until we found one with training error zero. The smaller the set size  $H(\mathcal{S})$  of global minima relative to  $H$ , the longer it takes. For this weight vector we then measured the corresponding true error (red dot) with the test data set. This was repeated 100 times for 30 different training sets  $\mathcal{S}$ , respectively, and the results are shown in the figure right next to the histogram (B1). By counting the number  $L$  of random weight vectors we have to draw to obtain zero training error 100 times,  $100/L$  gives us an estimation of  $H(\mathcal{S})/H$  for the given training set  $\mathcal{S}$ . This value can be found on the x-axis. As can be seen, the set size  $H(\mathcal{S})$  of global minima varies by more than a factor of 20 for the 30 different training sets of the same size  $n = 10$ . On the y-axis the test error is marked for each instant of zero training error (red dots). For a given training set  $\mathcal{S}$ , the fraction of red dots above a given  $\varepsilon$  corresponds to  $b_\varepsilon(\mathcal{S})$ . Interestingly,  $b_\varepsilon(\mathcal{S})$  does not correlate with  $H(\mathcal{S})$ . But then equality (6) is valid and the mean fraction of "bad" global minima within the set of all global minima is determined by the shape of  $D(E)$ . Of course, this experiment is not a comprehensive analysis, but indicates that the assumption of Theorem 1 makes sense.

On the right (C1) we see the distribution of the test errors at randomly found global minima of random training sets. For each  $n$ , the distribution of the test errors along the y-axis corresponds to the density function  $Q_n(E)$  in Equation (9). We obtained this by taking a randomly chosen training data set, and then randomly sampled weight vectors from the unit hypersphere until we found one with training error zero on this set. Then we determined the corresponding test error (red dot) with the test data set and took the next randomly chosen training data set. For each  $n$  this was repeated 1,000 times (1,000 red dots for each  $n$ ). The box-plots show, that already for  $n = 30$  more than 75% of the training error zero solutions provide test (true) errors of less than 0.2, i.e., for  $n = 30$  we have  $\langle b_{\varepsilon=0.2}(\mathcal{S}) \rangle = 0.25$ . In only one of the 1,000 trials there is a test error slightly above 0.4. "Bad" global minima are quickly becoming rare on the unit hypersphere.

The second row of Fig. 1 shows the results of the network with one hidden layer and 100 hidden units. This network has ten times as many weights as the previous network with 10 hidden units. Nevertheless, the shape of the density of classifiers  $D(E)$  (A2) hardly deviates from the  $D(E)$  of the much smaller network (A1). Again,  $H_\varepsilon(\mathcal{S})/H(\mathcal{S})$  does not correlate with  $H(\mathcal{S})$  (B2). Then (6) is valid and with (10) we have  $Q_n(E) \propto (1 - E)^n D(E)$ . Hence, since the

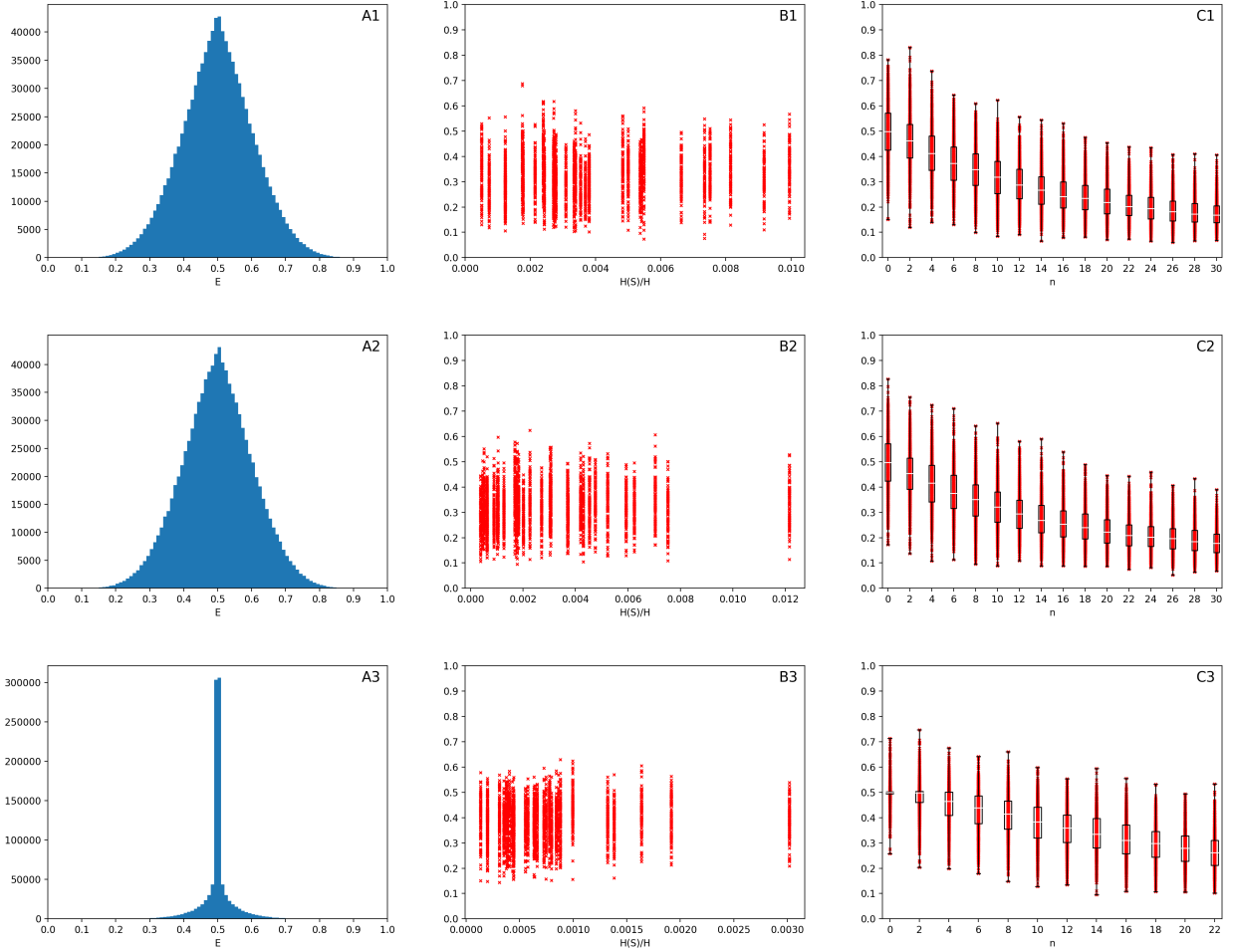


Figure 1: Experiments with two Gaussians in 10 dimensions, classified by three different networks from top to bottom. The shape of the density of classifiers  $D(E)$  (left column) of the first two networks hardly deviate, in spite of 10 times more weights in A2 than in A1. The red dots in the middle and right column show test errors. The fraction of "bad" solutions  $b_\varepsilon(S)$ , i.e., red dots above a given  $\varepsilon$ , does not correlate with  $H(S)$  (middle column). Then the mean distribution of the test (true) error is determined by the shape of  $D(E)$ , and the average fraction of "bad" solutions converges to zero (right column). Since A1 and A2 have more or less the same shape, also C1 and C2 are more or less identical.

density of classifiers  $D(E)$  of the large and the small network have more or less the same shape, also Figs. C1 and C2 are more or less identical. As for the ten times smaller network, already for  $n = 30$  in about 75% of the cases one ends up with a test error of less than 0.2, and in none of the 1,000 trials there is a test error above 0.4.

In the third row of Fig. 1 we see the density of classifiers  $D(E)$  for the network with ten hidden layers with ten neurons each and 1,020 weights (A3). The large peak at  $E = 0.5$  stems from weight configurations where the classifier output is always the same class, independent from the input. The classifiers  $h$  which correspond to these weight configurations are ruled out immediately as soon as training data from both classes occur, since then these  $h$  do not provide zero training error and do not belong to the global minimum. Again,  $H_\varepsilon(S)/H(S)$  does not seem to correlate with  $H(S)$  (B3) and, hence,  $Q_n(E) \propto (1 - E)^n D(E)$  is valid. With  $D(E)$  having a different shape as in the two cases before, also Fig. C3 looks differently now. It converges more slowly, and the peak of  $D(E)$  resolves with increasing  $n$ , as can be seen from the increasing box. For example, for  $n = 2$  in half of the training data instances the training data are from the same class and there still are solutions from the peak with  $E = 0.5$ . We stopped with  $n = 22$ , since the time to find zero training error solutions by random sampling started to take too much time

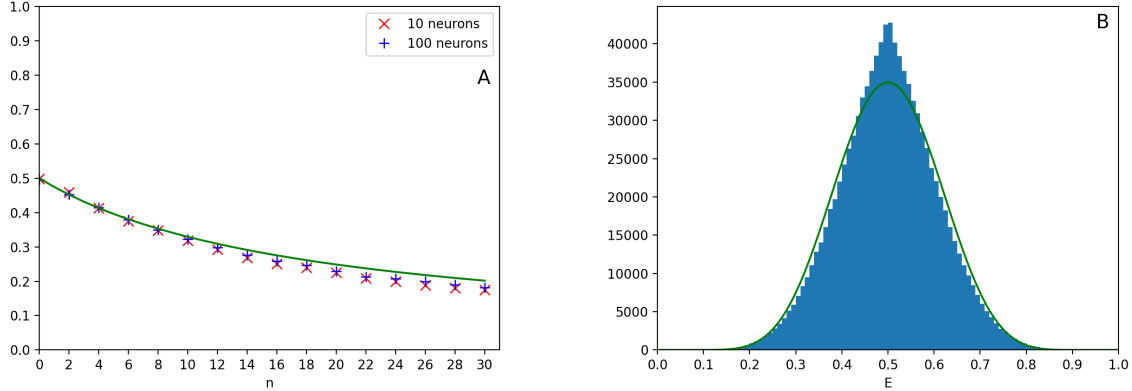


Figure 2: The mean test errors of the two networks with one hidden layer and 10 and 100 hidden units, respectively, on the synthetic data set for increasing  $n$  (crosses in A). The values of both networks match surprisingly well. The bell-shaped curve in B approximates the measured  $D(E)$  of the network with 10 hidden units (taken from Fig. 1 A1). From this bell-shaped curve as a quantitative description of  $D(E)$  the "learning curve" (16) is derived, which is shown in A.

In Fig. 2A we plot the average test error, which corresponds to  $\langle E_n \rangle_{\mathfrak{S}}$  in (11), of the small and the large one hidden-layer network for different  $n$ , taken from the values in C1 and C2 of Fig. 1. Both networks are over-parameterized, and the larger network is ten times as large as the smaller one, but nevertheless the mean test errors are more or less the same. We claim that this is due to  $D(E)$  of both networks having the same shape and Equations (11) and (10) being valid. The fraction of "bad" solutions quickly decays in both networks, in spite of being over-parameterized, and the ten times larger network does not need more training data. In Fig. 2B we approximate the shape of  $D(E)$  by

$$D(E) \propto (E - E_{min})^\alpha (1 - E_{min} - E)^\alpha$$

for  $E_{min} \leq E \leq 1 - E_{min}$ , otherwise  $D(E) = 0$ .  $D(E)$  is symmetric with a maximum at  $E = 0.5$  and decays to zero for  $E = E_{min}$  and  $E = 1 - E_{min}$ . Fig. 2B depicts the measured  $D(E)$  of the network with ten hidden units from Fig. 1 A1, for which  $\alpha = 8$  is taken as a fit. As shown in the Appendix, with (11) and (10) we obtain

$$\langle E_n \rangle_{\mathfrak{S}} \approx E_{min} + \frac{0.5 - E_{min}}{1 + \frac{n}{2(1+\alpha)}}. \quad (12)$$

As required, for  $n = 0$  we obtain  $\langle E_n \rangle_{\mathfrak{S}} = 0.5$ . For increasing  $n$ , the mean true error  $\langle E_n \rangle_{\mathfrak{S}}$  converges to its minimal possible value  $E_{min}$  with  $\mathcal{O}(\alpha/n)$ . In Fig. 2A, this "learning curve" is plotted for  $\alpha = 8$  and  $E_{min} = 0.0228$ . Except for slight deviations, which are not surprising with the various approximations, it supports the theoretically derived relation between  $D(E)$  and  $\langle E_n \rangle_{\mathfrak{S}}$ .

## 4.2 Data set from MNIST

In Fig. 3 we show the results of the same experiments with real data. We took the digits 1 and 2 of the MNIST data set as the two classes to be classified. Each digit image has a size of  $28 \times 28$  pixels and thus the input dimension is 784. We used the same network structure as before, in one case with no hidden layer, i.e., only two leaky output ReLUs, one for each class, and in the other case a one-hidden layer MLP with 10 hidden leaky ReLUs and two leaky output ReLUs. In the first case, the classifier has 1,568 weights, and in the second case 7,860 weights. The training data sets were randomly drawn from a set of 6,000 images of each digit, respectively. These images were taken from the MNIST training set. For testing, 900 images of each digit were taken from the MNIST test set.

The results look very much like in Fig. 1 for the synthetic data. In the first row of Fig. 3, the results without hidden layer and 1.568 weights and in the second row the results with ten hidden units and 7.860 weights are shown. From left to right we see the density of classifiers  $D(E)$ , the test whether  $b_\epsilon(\mathcal{S})$  and  $H(\mathcal{S})$  correlate, and the distribution of test errors at global minima of the training error for different  $n$ . For  $n > 34$  and  $n > 24$ , respectively, it started to take too much computing time to find zero training error solutions by random sampling and we stopped.

In both cases, the classifiers are highly over-parameterized for these small training data sets, but nevertheless good solutions quickly dominate. Again, the fraction of "bad" global minima  $b_\epsilon(\mathcal{S})$  does not correlate with the magnitude of

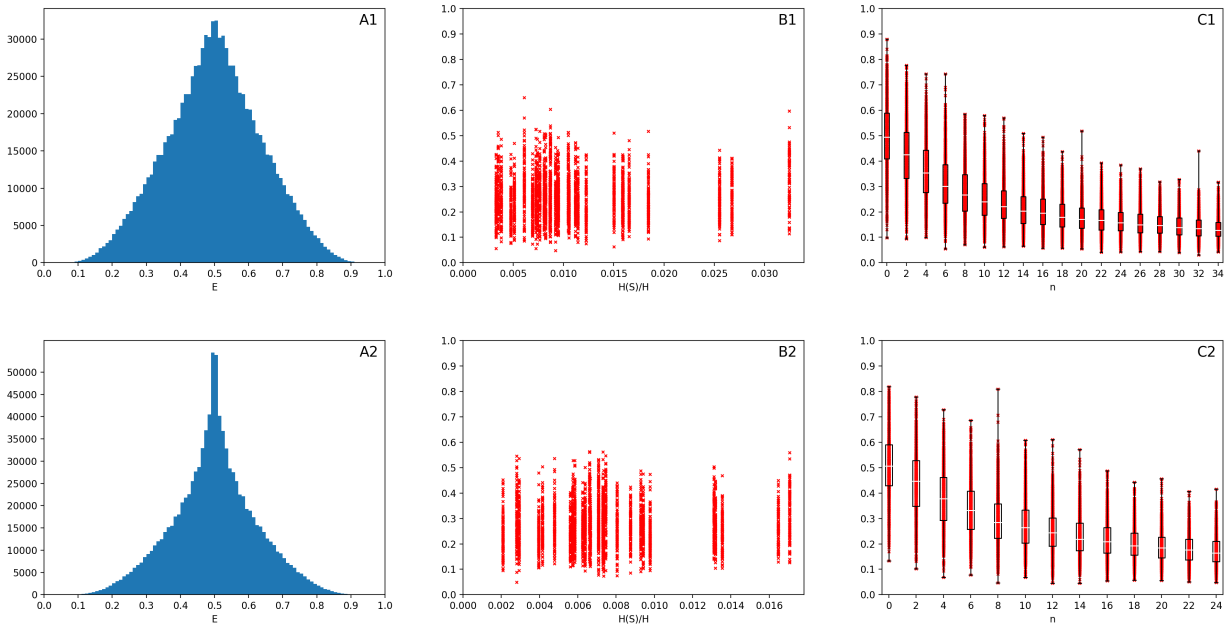


Figure 3: Classification of the two digits 1 and 2 of the MNIST data set with two output ReLUs (first row) and with one hidden layer with 10 hidden ReLUs and two output ReLUs (second row). Left the density of classifiers  $D(E)$  and right the distribution of test errors (red dots) for increasing number of training data  $n$ . In the middle, experimental tests with  $n = 10$ , demonstrating that the fraction of classifiers with a true (test) error (red dots) larger than a given  $\varepsilon$  within the solution set of zero training error does not correlate with size  $H(S)$  of this solution set.

the global minima set  $H(S)$ . Without correlation, the average distribution of the test (true) error for randomly found global minima (C1 and C2), i.e., the density function  $Q_n(E)$ , is determined by  $D(E)$ . For both networks, already for  $n = 24$  about 75% of all test errors are below 0.2. Instead of being wrong in every second case, after only 24 training samples 75% of the networks with training error zero make less than one mistake in five cases.

In Fig. 4A, we plot the mean test error  $\langle E_n \rangle$  of the two networks for different  $n$ , taken from the values in C1 and C2 of Fig. 3. Both networks are over-parameterized, and the larger network is five times as large as the smaller one, but again the mean test errors are more or less the same. In B we draw the  $D(E)$  of the larger network in blue onto the  $D(E)$  of the smaller one in red. Since both deviate only slightly, also the mean test errors match well.

### 4.3 VGG and ResNet and Caltech101

Finally, we take a look at very large Deep Networks. In [6] was shown that a VGG19 net with 140 million weights is able to learn to discriminate airplanes and motorcycles on images from the Caltech101 dataset [24] up to 95% accuracy trained with only 20 examples from each class. This extremely over-parameterized network was initialized randomly and then trained by stochastic gradient descent up to training error zero without any regularization. Fig. 5A shows these results adapted from [6]. With 200 training data the test accuracy is almost 100% despite complete over-fitting and memorizing the training data.

We explain these results by "bad" solutions being rare in the set of training error zero solutions. Therefore, an ERM algorithm like stochastic gradient descent should very likely end up in a good solution also without regularization. We test our hypotheses like in the previous sections. Again, due to the positive homogeneity of the VGG19 net each classifier function realized by VGG19 corresponds to a point on the unit hypersphere in the weight space. We uniformly draw random weights from this sphere, and if the corresponding classifier function has zero training error we determine its test accuracy. The training examples are drawn from 798 motorbike and aircraft images from Caltech101, always the same number for each class, analog to the experiments in Fig. 5A. The rest of the images are used for determining the test accuracy. Like in Fig. 5A we perform the same experiment also for ResNet18, which has 11, 2 million parameters - more than ten times less than VGG19.



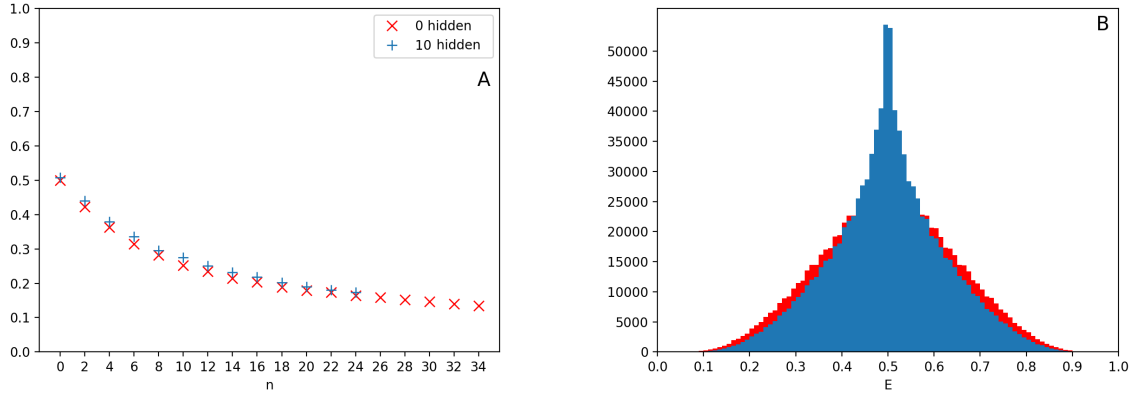


Figure 4: The mean test errors of the two networks on the digits 1 and 2 of the MNIST data set for increasing  $n$  (crosses in A). Again, the values of both networks match surprisingly well. In B, the  $D(E)$  of the larger network (blue) is drawn onto the  $DE$  of the smaller one (red). The deviations are small, resulting in small deviations of the mean test errors in A.

Fig. 5B shows the results for up to 10 samples per class (for larger  $n$  it became too computationally expensive). For each  $n$  we randomly drew weights until we reached 100 zero training error solutions. Fig. 5B shows the mean of the corresponding test accuracies and their variances. To find zero training error solutions required several million trials for larger  $n$ . Interestingly, on average it required much more trials for ResNet18 than for VGG19. Already for  $n = 10$  the training error zero solutions of VGG19 have a mean test accuracy of 75%. An extrapolation to  $n = 20$  leads to the range of VGG19 in Fig. 5A. Also ResNet18 being worse than VGG19 in spite of being ten times smaller corresponds to Fig. 5A. Both is very well in line with our hypothesis.

## 5 Discussion

Experiments have shown that highly over-parameterized classifiers do consistently learn, also without any explicit regularization, and despite "memorizing" the training data up to zero training error. This is in contrast to traditional machine learning wisdom, which is shaped by traditional learning theory based on uniform convergence. There, it is required (with high probability) that the generalization gap is uniformly small, i.e., that there is no "bad" classifier within the set of possible solutions for which the true and the training error differ too much. In contrast, we explain the observed learning of over-parameterized classifiers by claiming that the fraction of "bad" classifiers within the set of all possible solutions with zero training error becomes small (with high probability) as the number of training samples grows. This is much less than uniform convergence, where this fraction of "bad" classifiers must be zero, and can be achieved with much less training data. The smaller the fraction of "bad" classifiers, the easier it is for the ERM algorithm to find a good solution.

We can mathematically prove our claim with the sufficient condition that the fraction of "bad" classifiers within the set of global minima does not correlate negatively with the size of the set of global minima. Then, the fraction of "bad" classifiers becomes small exponentially with the number of training samples. We introduced the density of classifiers (DOC) at a true error  $E$  analogous to the density of states (DOS) at a certain energy in physical systems. The DOC depends on the set of classifier functions and the classification problem, and it determines the bound for the fraction of "bad" classifiers. In this sense, the DOC is the main property of a given classifier/problem case. Since its shape (i.e., the normalized DOC) is important, it does not depend on the capacity of the classifier or the number of parameters. Increasing the absolute density values by increasing the capacity of the classifier function set may keep the normalized DOC invariant, or may even improve it, as observed in many experiments.

We evaluated our claim experimentally on a synthetic data set and a subset of MNIST with three and two different network architectures and network sizes, respectively. We determined the DOC and the global minima sets by random sampling. In all cases, we indeed could not see any correlation of the fraction of "bad" classifiers within the global minima set and the size of the global minima set, at least not for the given settings. In these cases, the average fraction of "bad" classifiers is determined by the DOC. This could be verified experimentally. The experiments also showed that the DOC does not necessarily depend on the complexity and size of the classifier. Networks with ten times as many parameters had similar DOCs, and therefore their fraction of "bad" minima also decayed similarly, in agreement

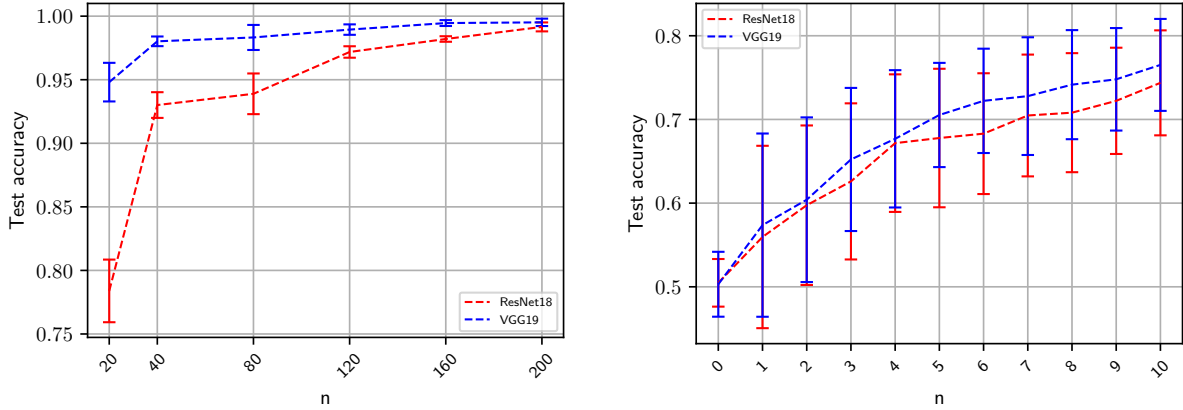


Figure 5: The left plots are adapted from [6] and show the mean test accuracies (and variances) in classifying motorcycles and airplanes on images from the Caltech101 dataset with VGG19 and ResNet18, respectively. Both networks are trained with stochastic gradient descent up to training error zero. To the right we see the mean test accuracies and their variances of solutions with zero error on the training data set obtained by random sampling. Good solutions quickly dominate within the set of zero training error solutions, and as with gradient descent the more than ten times larger VGG19 performs better than ResNet18.

with the mathematical framework we developed. Finally, we applied our framework to VGG19 and ResNet18, two Convolutional Neural Networks with millions of parameters. The observed increase of the fraction of good solutions with increasing number of training data is able to explain the good generalization of these networks observed in highly over-parameterized settings. It does not require any regularization, neither explicit nor implicit.

Of course, (stochastic) gradient descent as the standard ERM algorithm used for learning does not necessarily end up in each of the global minima with equal probability. It is influenced by many factors like initialization, structure of the error landscape, learning rates etc.. Therefore, unlike for random sampling, the probability to end up in a "bad" solution is not exactly given by the fraction of "bad" solutions. Nevertheless, in our experiments with VGG19 and ResNet18, the stochastic gradient descent results were in accordance with the random sampling results. Gradient descent would have to „exponentially“ favor "bad" solutions to end up in the tiny fraction of "bad" solutions. Traditional machine learning wisdom thought the other way round, that good solutions are rare, and that it needs a lot of guidance (e.g. regularization) to find them and to not end up in a "bad" solution. One would expect that these measures rather further increase the probability to end up in a good solution.

In our theory we required that there is no negative correlation between the fraction of "bad" classifiers within the set of global minima and the set size of global minima. In our experiments, there appeared to be no correlation for the settings we evaluated. For the theory to be complete, it remains an open corner stone under what conditions with respect to the mathematical structure of the classifier and the classification problem there is no negative or even no correlation. It is a macroscopic structural behavior of the classifier/problem setting. Perhaps this is related to high over-parameterization, or it is related to aspects of the structure of Neural Networks as a special case of a classifier. This remains an interesting open question for future work.

Our results suggest working with over-parameterized classifiers, contrary to the old rules not to do so. This may even be advantageous. Problems like "over-fitting" or tricks like "early stopping" are no longer an issue. Indeed, in practice, over-parameterized classifiers are already widely used.

## Acknowledgement

We thank Christoph Linse for discussions and providing the graphs in Figure 5.

## References

- [1] A. Krizhevsky, I. Sutskever, and G. Hinton, "Imagenet classification with deep convolutional neural networks," *Neural Information Processing Systems*, vol. 25, 01 2012.

- 
- [2] J. Devlin, M. Chang, K. Lee, and K. Toutanova, “BERT: pre-training of deep bidirectional transformers for language understanding,” *CoRR*, vol. abs/1810.04805, 2018.
  - [3] V. Mnih, K. Kavukcuoglu, D. Silver, A. A. Rusu, J. Veness, M. G. Bellemare, A. Graves, M. Riedmiller, A. K. Fidjeland, G. Ostrovski, S. Petersen, C. Beattie, A. Sadik, I. Antonoglou, H. King, D. Kumaran, D. Wierstra, S. Legg, and D. Hassabis, “Human-level control through deep reinforcement learning,” *Nature*, vol. 518, pp. 529–533, Feb. 2015.
  - [4] C. Zhang, S. Bengio, M. Hardt, B. Recht, and O. Vinyals, “Understanding deep learning requires rethinking generalization,” 2017.
  - [5] M. Belkin, D. Hsu, S. Ma, and S. Mandal, “Reconciling modern machine-learning practice and the classical bias–variance trade-off,” *Proceedings of the National Academy of Sciences*, vol. 116, p. 201903070, 07 2019.
  - [6] C. Linse and T. Martinetz, “Large neural networks learning from scratch with very few data and without explicit regularization,” *15th International Conference on Machine Learning and Computing (ICMLC)*, 2023.
  - [7] V. N. Vapnik, *Statistical Learning Theory*. Wiley-Interscience, 1998.
  - [8] P. L. Bartlett and S. Mendelson, “Rademacher and gaussian complexities: Risk bounds and structural results.,” *J. Mach. Learn. Res.*, vol. 3, pp. 463–482, 2002.
  - [9] B. Neyshabur, S. Bhojanapalli, D. McAllester, and N. Srebro, “Exploring generalization in deep learning,” in *NIPS*, 2017.
  - [10] A. Brutzkus, A. Globerson, E. Malach, and S. Shalev-Shwartz, “SGD learns over-parameterized networks that provably generalize on linearly separable data,” in *International Conference on Learning Representations*, 2018.
  - [11] D. Soudry, E. Hoffer, M. S. Nacson, S. Gunasekar, and N. Srebro, “The implicit bias of gradient descent on separable data,” *Journal of Machine Learning Research*, vol. 19, no. 70, pp. 1–57, 2018.
  - [12] B. Neyshabur, R. Tomioka, and N. Srebro, “Norm-based capacity control in neural networks,” in *Proceedings of the 28th Conference on Learning Theory (COLT)*, vol. PMLR 40, pp. 1376–1401, 2015.
  - [13] P. Bartlett, D. Foster, and M. Telgarsky, “Spectrally-normalized margin bounds for neural networks,” *Advances in Neural Information Processing Systems*, vol. 30, pp. 6241–6250, 2017.
  - [14] N. Golowich, A. Rakhlin, and O. Shamir, “Size-independent sample complexity of neural networks,” in *COLT*, 2018.
  - [15] S. Arora, R. Ge, B. Neyshabur, and Y. Zhang, “Stronger generalization bounds for deep nets via a compression approach,” in *Proceedings of the 35th International Conference on Machine Learning*, pp. 254–263, 2018.
  - [16] Y. Li and Y. Liang, “Learning overparameterized neural networks via stochastic gradient descent on structured data,” in *Advances in Neural Information Processing Systems* (S. Bengio, H. Wallach, H. Larochelle, K. Grauman, N. Cesa-Bianchi, and R. Garnett, eds.), vol. 31, Curran Associates, Inc., 2018.
  - [17] V. Nagarajan and Z. Kolter, “Deterministic PAC-bayesian generalization bounds for deep networks via generalizing noise-resilience,” in *International Conference on Learning Representations*, 2019.
  - [18] B. Neyshabur, Z. Li, S. Bhojanapalli, Y. LeCun, and N. Srebro, “The role of over-parametrization in generalization of neural networks,” in *International Conference on Learning Representations*, 2019.
  - [19] C. Wei and T. Ma, “Data-dependent sample complexity of deep neural networks via lipschitz augmentation,” in *NeurIPS*, 2019.
  - [20] T. Liang, T. Poggio, A. Rakhlin, and J. Stokes, “Fisher-rao metric, geometry, and complexity of neural networks,” in *Proceedings of Machine Learning Research*, pp. 888–896, 2019.
  - [21] H. N. Mhaskar and T. A. Poggio, “An analysis of training and generalization errors in shallow and deep networks,” *Neural Networks*, vol. 121, pp. 229–241, 2020.
  - [22] Y. Jiang, B. Neyshabur, H. Mobahi, D. Krishnan, and S. Bengio, “Fantastic generalization measures and where to find them,” *CoRR*, vol. abs/1912.02178, 2019.
  - [23] V. Nagarajan and J. Z. Kolter, “Uniform convergence may be unable to explain generalization in deep learning,” pp. 11611–11622, 2019.
  - [24] F.-F. Li, M. Andreeto, M. Ranzato, and P. Perona, “Caltech 101,” Apr 2022.
  - [25] L. G. Valiant, “A theory of the learnable,” in *STOC '84*, 1984.

## A Appendix

### Proofs

#### Lemma 1:

*Proof.* For a given  $h$ , the loss  $L(y, h(x))$  is a binomial random variable assuming the values 0 or 1 for training data drawn i.i.d. from  $P(x, y)$ . The probability for  $h$  to be a consistent classifier with  $L(y_i, h(x_i)) = 0$  for each  $(x_i, y_i) \in \mathcal{S}$  is  $(1 - E(h))^n$  (see also PAC learning [25]). With the indicator function  $\mathbf{1}_{\mathcal{H}_\varepsilon(\mathcal{S})}(h)$ , which is one for  $h \in \mathcal{H}_\varepsilon(\mathcal{S})$  and otherwise zero, we obtain

$$\begin{aligned}
 \langle H_\varepsilon(\mathcal{S}) \rangle &= \left\langle \sum_{h \in \mathcal{H}_\varepsilon} \mathbf{1}_{\mathcal{H}_\varepsilon(\mathcal{S})}(h) \right\rangle_{\mathcal{S}} \\
 &= \sum_{h \in \mathcal{H}_\varepsilon} \langle \mathbf{1}_{\mathcal{H}_\varepsilon(\mathcal{S})}(h) \rangle_{\mathcal{S}} \\
 &= \sum_{h \in \mathcal{H}_\varepsilon} (1 - E(h))^n \\
 &\leq H_\varepsilon (1 - (E_{\min} + \varepsilon))^n.
 \end{aligned} \tag{13}$$

□

#### Corollary 1:

*Proof.* We show that for any  $a > 1$  and  $0 < \varepsilon \leq 1 - E_{\min}$

$$\frac{\langle H_\varepsilon(\mathcal{S}) \rangle}{\langle H(\mathcal{S}) \rangle} \leq \frac{1}{g_{\varepsilon/a}} e^{-(1-1/a)\varepsilon n}. \tag{14}$$

Corollary 2.2 is the special case for  $a = 2$ .

With equation (13) we obtain

$$\begin{aligned}
 \frac{\langle H_\varepsilon(\mathcal{S}) \rangle}{\langle H(\mathcal{S}) \rangle} &= \frac{\sum_{h \in \mathcal{H}_\varepsilon} (1 - E(h))^n}{\sum_{h \in \mathcal{H}} (1 - E(h))^n} \\
 &\leq \frac{H_\varepsilon (1 - (E_{\min} + \varepsilon))^n}{\sum_{h \in \mathcal{H}} (1 - E(h))^n}.
 \end{aligned}$$

For any  $a > 1$  we obtain for the denominator

$$\begin{aligned}
 \sum_{h \in \mathcal{H}} (1 - E(h))^n &\geq \sum_{h \in \mathcal{H}/\mathcal{H}_{\varepsilon/a}} (1 - E(h))^n \\
 &\geq (H - H_{\varepsilon/a}) (1 - (E_{\min} + \varepsilon/a))^n.
 \end{aligned}$$

But then

$$\frac{\langle H_\varepsilon(\mathcal{S}) \rangle}{\langle H(\mathcal{S}) \rangle} \leq \frac{H_\varepsilon (1 - (E_{\min} + \varepsilon))^n}{(H - H_{\varepsilon/a}) (1 - (E_{\min} + \varepsilon/a))^n}.$$

For  $\varepsilon = 1 - E_{\min}$ , the r.h.s. is zero. For  $0 < \varepsilon < 1 - E_{\min}$ , the r.h.s. can be written as

$$\begin{aligned}
 \frac{\langle H_\varepsilon(\mathcal{S}) \rangle}{\langle H(\mathcal{S}) \rangle} &\leq \frac{H_\varepsilon}{H - H_{\varepsilon/a}} e^{-n(\ln(1 - (E_{\min} + \varepsilon/a)) - \ln(1 - (E_{\min} + \varepsilon)))} \\
 &\leq \frac{1}{g_{\varepsilon/a}} e^{-n(\ln(1 - (E_{\min} + \varepsilon/a)) - \ln(1 - (E_{\min} + \varepsilon)))}.
 \end{aligned}$$

With the Taylor-expansions  $\ln(1 - x) = -x - x^2/2 - x^3/3 - \dots$  it is easy to see that

$$\ln(1 - (E_{\min} + \varepsilon/a)) - \ln(1 - (E_{\min} + \varepsilon)) \geq (1 - 1/a)\varepsilon,$$

which concludes the proof. □

**Theorem 1:**

*Proof.* Let  $\mathbf{S}$  denote the set of all  $S$ , and  $\hat{\mathbf{S}}$  denote the set of all  $S$  with  $H(S) > 0$ . Each  $S$  occurs with a probability  $P(S)$ , determined by  $P(x, y)$ . We have

$$p = \int_{\hat{\mathbf{S}}} P(S) dS \leq \int_{\mathbf{S}} P(S) dS = 1.$$

$p$  is the probability, that  $H(S) > 0$ .

If  $b_\varepsilon(S)$  does not correlate negatively with  $H(S)$  for  $S \in \hat{\mathbf{S}}$ , then per definition

$$\langle b_\varepsilon(S)H(S) \rangle_{\hat{\mathbf{S}}} - \langle b_\varepsilon(S) \rangle_{\hat{\mathbf{S}}} \langle H(S) \rangle_{\hat{\mathbf{S}}} \geq 0.$$

Equality with zero corresponds to non-correlation. With  $b_\varepsilon(S)H(S) = H_\varepsilon(S)$  per definition, it directly follows

$$\langle b_\varepsilon(S) \rangle_{\hat{\mathbf{S}}} \leq \frac{\langle H_\varepsilon(S) \rangle_{\hat{\mathbf{S}}}}{\langle H(S) \rangle_{\hat{\mathbf{S}}}}. \quad (15)$$

Since  $H(S) = 0$  for  $S \in \mathbf{S}/\hat{\mathbf{S}}$ , we have

$$\begin{aligned} \langle H(S) \rangle_{\hat{\mathbf{S}}} &= \frac{1}{p} \int_{\hat{\mathbf{S}}} H(S) P(S) dS \\ &= \frac{1}{p} \int_{\mathbf{S}} H(S) P(S) dS \\ &= \frac{1}{p} \langle H(S) \rangle \end{aligned}$$

and, analogously (if  $H(S) = 0$ , then also  $H_\varepsilon(S) = 0$ ),

$$\langle H_\varepsilon(S) \rangle_{\hat{\mathbf{S}}} = \frac{1}{p} \langle H_\varepsilon(S) \rangle.$$

But then

$$\frac{\langle H_\varepsilon(S) \rangle_{\hat{\mathbf{S}}}}{\langle H(S) \rangle_{\hat{\mathbf{S}}}} = \frac{\langle H_\varepsilon(S) \rangle}{\langle H(S) \rangle}.$$

Together with (15) and Corollary 2.2 we obtain

$$\langle b_\varepsilon(S) \rangle_{\hat{\mathbf{S}}} \leq \frac{1}{g_{\varepsilon/2}} e^{-\frac{\varepsilon}{2}n}$$

and the Markov-inequality concludes the proof.  $\square$

**Approximation of the "learning curve"**

If  $D(E)$  can be described by

$$D(E) \propto (E - E_{min})^\alpha (1 - E_{min} - E)^\alpha,$$

with (11) and (10) we obtain for  $\langle E_n \rangle_{\hat{\mathbf{S}}}$  the expression

$$\begin{aligned} \langle E_n \rangle_{\hat{\mathbf{S}}} &= \frac{\int_0^1 E(1-E)^n D(E) dE}{\int_0^1 (1-E)^n D(E) dE} \\ &= \frac{\int_{E_{min}}^{1-E_{min}} E(1-E)^n (E - E_{min})^\alpha (1 - E_{min} - E)^\alpha dE}{\int_{E_{min}}^{1-E_{min}} (1-E)^n (E - E_{min})^\alpha (1 - E_{min} - E)^\alpha dE}. \end{aligned}$$

Since  $E_{min}$  is small, we can replace  $(1-E)^n \approx (1-E_{min}-E)^n$ , which allows to solve the integrals in closed form and the expression reduces to

$$\begin{aligned} \langle E_n \rangle_{\hat{\mathbf{S}}} &\approx \frac{\int_{E_{min}}^{1-E_{min}} E(E - E_{min})^\alpha (1 - E_{min} - E)^{\alpha+n} dE}{\int_{E_{min}}^{1-E_{min}} (E - E_{min})^\alpha (1 - E_{min} - E)^{\alpha+n} dE} \quad \text{for small } E_{min} \\ &\approx E_{min} + \frac{0.5 - E_{min}}{1 + \frac{n}{2(1+\alpha)}}. \end{aligned} \quad (16)$$